The Rqc2/Tae2 subunit of the Ribosome-Associated Quality Control (RQC) complex marks ribosome-stalled nascent polypeptide chains for aggregation

Ryo Yonashiro [1]*, Erich B. Tahara [1]*†, Mario H. Bengtson [1]†, Maria Khokhrina [2], Holger Lorenz [2], Kai-Chun Chen [1], Yu Kigoshi-Tansho [1], Jeffrey N. Savas [3,]†, John R. Yates III [3], Steve A. Kay [1], Elizabeth A. Craig [4], Axel Mogk [2], Bernd Bukau [2], and Claudio A.P. Joazeiro [1,5 §]

[1] Department of Cell and Molecular Biology, The Scripps Research Institute, 10550 N Torrey Pines Rd, La Jolla, California 92037, USA.

[2] Zentrum für Molekulare Biologie der Universität Heidelberg (ZMBH), Deutsches Krebsforschungszentrum (DKFZ), DKFZ-ZMBH Alliance, Im Neuenheimer Feld 282, Heidelberg D-69120, Germany.

[3] Department of Chemical Physiology, The Scripps Research Institute, 10550 N Torrey Pines Rd, La Jolla, California 92037, USA.

[4] Department of Biochemistry, University of Wisconsin - Madison, 433 Babcock Dr, Madison, Wisconsin 53706, USA.

[5] Zentrum für Molekulare Biologie der Universität Heidelberg (ZMBH), Deutsches Krebsforschungszentrum (DKFZ)-ZMBH Alliance, Im Neuenheimer Feld 282, Heidelberg D-69120, Germany.

† Present addresses: University of São Paulo, São Paulo, Brazil (E.B.T.); University of Campinas, São Paulo, Brazil (M.H.B.); Department of Neurology, Feinberg School of Medicine, Northwestern University, Chicago, IL 60611, USA (J.N.S.).

§ Correspondence to: joazeiro@scripps.edu.

* These authors contributed equally to this work.

Author Information. The authors declare no competing financial interests. Correspondence and requests for materials should be addressed to C.J. (joazeiro@scripps.edu).

Abstract

Ribosome stalling during translation can potentially be harmful, and is surveyed by a conserved quality control pathway that targets the associated mRNA and nascent polypeptide chain (NC). In this pathway, the ribosome-associated quality control (RQC) complex promotes the ubiquitylation and degradation of NCs remaining stalled in the 60S subunit. NC stalling is recognized by the Rqc2/Tae2 RQC subunit, which also stabilizes binding of the E3 ligase, Listerin/Ltn1. Additionally, Rqc2 modifies stalled NCs with a carboxy-terminal, Ala- and Thr-containing extension—the "CAT tail." However, the function of CAT tails and fate of CAT tail-modified ("CATylated") NCs has remained unknown. Here we show that CATylation mediates formation of detergent-insoluble NC aggregates. CATylation and aggregation of NCs could be observed either by inactivating Ltn1 or by analyzing NCs with limited ubiquitylation potential, suggesting that inefficient targeting by Ltn1 favors the Rqc2-mediated reaction. These findings uncover a translational stalling-dependent protein aggregation mechanism, and provide evidence that proteins can become specifically marked for aggregation.

Introduction

Under various circumstances, translating ribosomes can halt NC elongation and become stalled, such as upon translation of mRNA templates lacking stop codons, containing sequential suboptimal codons, or encoding homopolymeric Lys tracts [1-3]. Ribosome stalling poses a problem, as it can both reduce the pool of translation-competent ribosomes and give rise to aberrant—and potentially toxic—nascent polypptide chains (NCs). To prevent these undesirable consequences from taking place, stalled ribosomes are rescued by factors that split the subunits, releasing the mRNA (for degradation by the exosome), the 40S subunit, and the 60S subunit stalled with a nascent peptidyl-tRNA conjugate, which is then targeted by the RQC complex [1-3]. The RQC is minimally composed of the Ltn1 (Listerin in mammals), Rqc1, and Rqc2/Tae2 (NEMF in mammals) subunits [4-6]. How the RQC functions has only begun to be understood. According to the current model, Rqc2 first recognizes the stalled 60S and facilitates binding of the Ltn1 E3 ligase, which, in turn, ubiquitylates the aberrant NC [7-9]. Next, in a manner dependent on Rqc1, the Cdc48/VCP AAA ATPase and its ubiquitin-binding cofactors are recruited to the complex and facilitate NC delivery to the proteasome for degradation [5,6,10]. It has been recently discovered that Rqc2 can, in addition, recruit Ala- or Thr-loaded tRNA to promote the C-terminal elongation of stalled NCs in a template- and 40S ribosomal subunit-independent manner [8]. Such "CAT tails" have no defined sequence and are heterogeneous in length, forming a smear extending as much as 5 kDa above the unmodified reporter band in SDS-PAGE. The physiological relevance of this process has remained unclear, however, as so far it has only been reported for Ltn1- or Rqc1-deficient cells [8]. Moreover, the fate of CATylated NCs has remained unknown.

Results

Stalled translation can lead to the formation of nascent chain aggregates

We observed that, in *ltn1*Δ cells, in addition to the previously described increased steady-state levels and "CATylation" of stalling reporters [4,8], a fraction of those reporters migrated very slowly in gel electrophoresis, close to the loading well (**Figure 1A;** in the experiments presented, smears due to CATylation often run close to the unmodified reporter band, and can be more clearly observed with the smaller molecular weight reporters, PtnA-NS and GRR; see also below). The phenomenon was also observed with cells in which only Ltn1's E3-catalytic RING domain had been deleted (Ltn1 ΔR; **Figure 1A**, left panel) suggesting that it is prevented by Ltn1-mediated ubiquitylation under normal conditions.

We analyzed several stalling reporters that have been previously described. In one set, the reporters consist of a GFP-Flag-His3 fusion followed by a stop codon (K0), lacking stop codons (NS, for "nonstop"), or followed by a 12 Lys track and stop codons (K12) (**Figure 1A**, left panel, and [4,11]). Translation of NS and K12 reporters is believed to stall due to polyLys tract synthesis. In a second set of reporters, the Protein A ZZ domain (PtnA) is followed by a stop codon (STOP-Rz), by a wild type self-cleaving ribozyme sequence (NS-Rz), or by a mutant ribozyme (*rz*) (**Figure 1A**, middle panel, and [12]). In the case of the NS-Rz reporter mRNA, translating ribosomes stall as they reach the 3'end of the cleaved mRNA with no stop codons present; on the other hand, with the mutant *rz* reporter, the mRNA fails to be cleaved, allowing translation to proceed through an in-frame GFP sequence without stalling. In a third set of experiments, a GFP-12(Arg)-RFP fusion protein (GRR) was utilized (**Figure 1A**, right panel, and ref [11]). In this

89 case, stalling occurs as a result of the presence of multiple unpreferred Arg CGN codons [13].
90 Despite their unrelated encoded protein sequences and distinct stalling mechanisms, we were
91 able to observe slow-migrating species for all stalling reporters examined, but not their
92 respective parental controls (e.g., K0, STOP-Rz). The formation of slow-migrating reporter
93 species thus appears to be translational stalling-dependent.

94 We next investigated the nature of these high-molecular weight species. Slow migration was not
95 due to Ltn1-independent poly-ubiquitylation of stalling reporters, since migration was not shifted
96 after treatment with the deubiquitylating enzyme, Usp2 (**Figure 1—figure supplement 1A**; [14]).
97 We reasoned that those species might instead correspond to insoluble aggregates. Consistent
98 with this possibility, slow-migrating reporter species were efficiently sedimented by
99 centrifugation under conditions normally used to pellet protein aggregates (see, e.g., [15,16]), in
100 contrast to a soluble protein (Pgk1) or the bulk of high-molecular weight poly-ubiquitylated
101 proteins in the extract (**Figure 1B**).

102 The ability to observe aggregates of stalling reporter proteins by western-blot implies that those
103 aggregates are resistant to solubilization by boiling in 1% sodium dodecyl sulfate (SDS), as
104 samples for the experiments above were subjected to this treatment prior to gel running.
105 Resistance to ionic detergents is characteristic of ordered fibrillar structures such as the amyloid
106 formed by yeast prions or by expanded polyglutamine (polyQ) tracts (e.g., [17,18]). To our
107 knowledge, this is the first report of E3 dysfunction leading to formation of aggregates sharing
108 properties with amyloid.

109 However, in contrast to its effects on stalling reporters, deletion of *LTN1* failed to affect levels or
110 stimulate aggregation of a Huntingtin exon 1 polyQ-GFP reporter carrying either a disease-

111 associated expansion (Htt Q72) or a normal length tract (Htt Q25; **Figure 1—figure supplement**
112 **1B**; [19]). Thus, loss of Ltn1 function is not associated with the increased formation of protein
113 aggregates in general, but rather appears to be specifically associated with stalled NC
114 aggregation.

115 To further verify that ribosome stalling is required for NC aggregation, we took advantage of the
116 knowledge that the Hel2 protein is required for polybasic tract-mediated translational stalling [5].
117 Thus, in a *hel2*Δ background, ribosomes translating a 12-Lys tract in a stop codon-containing
118 reporter (K12) would be expected to translate through the tract, reach the stop codon, and
119 terminate translation normally, releasing the NC; on the other hand, the stalling of ribosomes
120 translating a *bona fide* non-stop mRNA (e.g., NS) would not be expected to be prevented by
121 *HEL2* deletion [5]. We thus asked what consequence *HEL2* deletion would have on reporter
122 aggregation. As predicted, the results in **Figure 1C** show that *HEL2* deletion efficiently
123 suppressed aggregation of K12—but not NS—in the *ltn1*Δ background.

124

125 **Rqc2-mediated modification of stalled nascent chains with CAT tails results in their**
126 **aggregation**

127 The formation of NC aggregates in Ltn1-deficient cells correlated with NC modification with
128 CAT tails. Furthermore, the low-complexity CAT tail sequences [8] are reminiscent of aggregate-
129 forming polyAla tracts [20]. We thus hypothesized that the aggregation of stalled NCs was
130 mediated by CAT tails.

Consistent with the hypothesis, stalled NC CATylation and aggregation were also observed in *rqc1*Δ cells (**Figure 2A**). The observation that *RQC1* deletion phenocopied *LTN1* deletion with regard to NC aggregation also implies that it is not a defect in Ltn1-mediated ubiquitylation *per se*—which is functional in the *rqc1*Δ background [5,6]—that causes aggregation (consistent with this interpretation, treatment of wild type yeast with the proteasome inhibitor MG132 led to stalling reporter accumulation without producing aggregates; **Figure 2—figure supplement 1A**). Rather, these results suggest that stalled NCs are driven towards CATylation and aggregation as a result of a defect in a step downstream of ubiquitylation but upstream of the proteasome, such as Cdc48/VCP recruitment [10].

Further correlation between CATylation and aggregation was obtained by inspecting the PtnA-Rz reporter in a Ltn1-deficient strain also lacking Rqc2—the results in **Figure 2A** show that, in the absence of CAT tails, NC aggregates also failed to form. We further examined the CAT tail requirement for NC aggregation by using *ltn1*Δ *rqc2*Δ strains expressing a stalling reporter and transformed with plasmids encoding either wild type Rqc2, or Rqc2 carrying a mutation in the highly conserved Asp98 residue. Asp98 is required for CAT tail synthesis but not for ribosome binding—in fact, the Rqc2 D98Y mutant is expressed normally and is fully competent to support Ltn1 function in *rqc2*Δ cells (**Figure 2—figure supplement 1B** and [8]). As predicted by the hypothesis, while overexpression of wild type Rqc2 led to the quantitative conversion of the stalling reporter into aggregated forms, the Rqc2 D98Y mutant was unable to promote stalling reporter aggregation (**Figure 2B**). Overexpression of wild type Rqc2 also led to more quantitative conversion of monomeric to CATylated and aggregated forms of the stalling reporter in *ltn1*Δ cells, suggesting that endogenous Rqc2 is limiting (**Figure 2C**). Moreover, differently from what we had observed for Hel2 (**Figure 1C**), the CAT tail synthesis requirement

for aggregation was evident with all stalling reporters examined, including NS (**Figure 2—figure supplement 1C**). Yet, this requirement appeared to be specific to stalling reporters, as *RQC2* deletion did not affect polyQ reporter aggregation (**Figure 2—figure supplement 1D**).

The hypothesis also predicted that hard-coding a CAT tail on a stop codon-containing reporter construct might bypass the requirements for both stalling and Rqc2 for protein aggregation. To test this possibility, we generated a construct in which a tract of 10 Ala-Thr repeats [(AT)10] was fused to the C-terminus of the control reporter K0 with the intent to mimic a CAT tail, followed by stop codons. The (AT)10 reporter has no stalling sequence, so its encoded protein is not expected to be a target of the RQC. As shown in **Figure 2D**, (AT)10, but not homopolymeric constructs with 20 Ala (A20) or 20 Thr (T20), was indeed able to form aggregates. Given that homopolymeric Ala tracts have been previously implicated in amyloid formation [20], we presume that this type of sequence may need to be longer in order to form aggregates under the conditions utilized here. Thus, the combination of Ala and Thr as found in CAT tails appears to be more prone to aggregate, which can be observed with a sequence as short as 20 amino acids long. These results suggest that, in addition to being required, CAT tails can also be sufficient for aggregate formation.

Arguing against the possibility of reporter aggregation being a post-lysis artifact, mixing *ltn1*Δ cells with K12-expressing *ltn1*Δ *rqc2*Δ cells immediately prior to cell lysis did not support aggregate formation (**Figure 2—figure supplement 1E**). In order to obtain further evidence for the formation of NC aggregates in intact cells, we examined the distribution of the GRR stalling reporter under fluorescence microscopy (**Figure 2E**). In the WT strain transformed with GRR, the low GFP signal was evenly distributed throughout the cytoplasm, with 1-3 local

accumulations of signal being observed; in contrast, *LTN1* deletion led to the appearance of numerous GFP *punctae*, characterized by foci with intense brightness over a low, diffuse cytosolic fluorescence background, in a third of cells [i.e., 15 out of 45 cells showing this phenotype; we note that aggregate formation in the *ltn1*Δ strain is limited by endogenous Rqc2 levels (see **Figure 2C** above)]. GFP *punctae* formation in *ltn1*Δ cells depended on Rqc2-mediated CATylation, as evidenced by the finding that the phenomenon could be suppressed by *RQC2* deletion (**Figure 2E**), and subsequently rescued by overexpression of Rqc2 wild type but not D98Y (**Figure 2F**). Thus, the appearance of GFP *punctae* in living cells correlated with the presence of protein aggregates in cell extracts.

The results presented so far indicate that NCs can be assembled into aggregates through a process triggered by ribosome stalling and requiring CAT tail synthesis by Rqc2. This implies that proteins can become "tagged" for aggregate assembly, and that this happens while nascent chains are still associated with the 60S subunit.

Sis1 association reveals endogenous stalled nascent chain aggregates

Because molecular chaperones are implicated in handling misfolded and aggregated proteins (e.g., [21-23]) we next examined the association of candidate chaperones with stalling reporters. Consistent with previous reports indicating that yeast amyloid aggregates are typically bound to the Hsp40/J protein, Sis1 (e.g., [24-26]), the binding of Sis1 to stalling reporters was readily apparent in extracts of a *ltn1*Δ strain (**Figure 3A** and **Figure 3—figure supplement 1A**). Other chaperones, such as Hsp70 Ssa1 and the Hsp40/J-protein Ydj1, also co-immunoprecipitated (co-IP'ed) with stalling reporters above background level but the differences were less marked and

appeared more variable. Consistent with these observations, analysis of chaperones co-IP'ed with the K12 stalling reporter expressed in a *ltn1*Δ strain by mass spectrometry uncovered Sis1 among the most abundant hits, and with the apparent highest signal-to-noise ratio [**Supplementary file 1 (Table SI)**]. In contrast to the conspicuous co-IP of Sis1 with stalling reporters in *ltn1*Δ cells, markedly less Sis1 was pulled down by anti-Flag antibody-conjugated beads from a *ltn1*Δ strain expressing no Flag-tagged stalling reporters, from a *ltn1*Δ strain expressing the K0 parental reporter, or from *rqc2*Δ or *ltn1*Δ *rqc2*Δ strains (**Figure 3A**). Thus, the Sis1 co-IP depended on stalling and on Rqc2, suggesting it binds stalled NCs *via* the CAT tails and/or aggregates.

Strikingly, a fraction of Sis1 itself exhibited slow-migrating species that were resistant to boiling in 1% SDS in *ltn1*Δ or *rqc1*Δ cells, but not in the *ltn1*Δ *rqc2*Δ strain (**Figure 3B**). The specificity of this phenomenon is underscored by the failure to observe similar slow migrating species for Ssa1 or Ydj1 (**Figure 3B**). Like stalled NC aggregates, those Sis1 species were unaffected by treatment with Usp2cc (**Figure 3—figure supplement 1B**). Moreover, slow-migrating Sis1 species could be pulled down along with an IP'ed stalling reporter (K12 Flag IP; **Figure 3—figure supplement 1C**), and their formation was dependent on Rqc2's ability to synthesize CAT tails (**Figure 3C**). Together, these results suggest that Sis1 tightly associates with stalled NC aggregates. Importantly, given that the formation of these Sis1 species was independent of ectopic expression of stalling reporters, these findings also provide evidence for aggregate formation by endogenous stalled NCs, and suggest that stalling reporter aggregation is not an artifact caused by their overexpression.

219 The above observations raised the question of whether Sis1 plays a role in NC aggregation.
220 Given that *SIS1* is an essential gene, to shed light onto this issue, stalling reporter aggregation
221 was examined in a *ltn1*Δ strain in which *SIS1* expression is under the tetO7 promoter, so it can be
222 turned off by treatment with doxycycline [24]. The results in **Figure 3D** show that the levels of
223 Sis1 in both free and aggregated forms were indeed reduced in response to doxycycline (left
224 panel), and that this was accompanied by a marked increase in steady-state levels of NC
225 aggregates (right panel). We also examined the effect of doxycycline in intact cells expressing
226 the GRR stalling reporter (**Figure 3E**). Consistent with the immunoblot data in **Figure 3D**, the
227 imaging results show that both the fraction of cells with GFP *punctae* and the number of *punctae*
228 per cell were increased in *ltn1*Δ Tet-Sis1 cells (**Figure 3E**). In contrast, such effects were modest
229 at best in *ltn1*Δ cells in which Sis1 expression is under its endogenous promoter and unaffected
230 by doxycycline treatment (**Figure 3E** and **Figure 3—figure supplement 2**).

231

232 **Evidence for stalled nascent chain modification with CAT tails and aggregation in wild**
233 **type cells**

234 NC CATylation has so far only been observed with mutant yeast strains harboring inactivating
235 mutations in Ltn1 or Rqc1, raising the issue of physiological relevance [8]. This observation
236 suggested it might also be possible to observe Rqc2-dependent effects in wild type cells by
237 utilizing stalling reporters less efficiently targeted by Ltn1—e.g., with fewer potential
238 ubiquitylation sites. To test this possibility, we generated reporters with all lysine residues
239 mutated to arginine ("K-less") and fused or not to the R12 stalling sequence.

One set of reporters was based on HA-tagged GFP K-less fused or not to 12 suboptimal Arg codons that cause ribosomal stalling (K-less R12). Cells transformed with GFP K-less or GFP K-less R12 constructs were analyzed for HA tag expression (**Figure 4A**). Remarkably, CATylation of the GFP K-less R12 reporter was readily evident in the wild type strain, as indicated by the presence of a smear immediately above the monomeric reporter band (lane 3), which was dependent both on Rqc2 (compare lanes 3 and 5) and on the R12 stalling sequence (compare lanes 2 and 3).

However, under the above conditions, the formation of aggregates with the GFP K-less R12 reporter was not observed (**Figure 4A**). We presume this could be due to a detection issue, since GFP K-less was expressed at lower steady-state levels compared to GFP, perhaps due to imperfect folding [27] (see shorter exposure; indeed, Rqc2- and stalling-dependent K-less reporter aggregates became evident in wild type cells treated with proteasome inhibitor and after concentrating the samples by affinity purification (**Figure 4—figure supplement 1**).

The formation of stalling reporter aggregates in wild type cells was more conspicuous when analyzing a different set of reporters, based on Protein A ZZ domain-Rz construct (described in **Figure 1A**). Wild type cells transformed with stop codon-containing controls or Rz-dependent stalling constructs were analyzed for PtnA expression (**Figure 4B**). Regardless of whether or not they contained lysines, PtnA-STOP-Rz reporters exhibited a similar expression pattern, consisting of a major band of the expected size of the PtnA ZZ domain (lanes 1 and 3). As observed in **Figure 1A**, the PtnA-NS-Rz construct additionally encoded a protein corresponding in size to the product of full-length, uncleaved PtnA-(Rz)-GFP (lane 2). In contrast, in wild type cells expressing the PtnA-NS-Rz K-less construct, a band corresponding to the PtnA ZZ domain was not evident; instead, smears corresponding to its CATylated and aggregated forms were

conspicuous (lane 4; compare to lane 2). We interpret this result as indicating that stalled NC encoded by the truncated PtnA-NS-Rz mRNA are normally targeted for degradation (compare lanes 1 and 2), but targeted for CATylation and aggregation if lysine ubiquitylation sites are not readily available. Furthermore, we conclude that Rqc2-dependent CATylation and aggregation of stalled NCs can both be observed in wild type cells with a functional RQC complex.

Discussion

Stalled NC metabolism has recently emerged as a paradigm for the understanding of co-translational quality control, and includes mechanisms for handling aberrant NCs along with their encoding mRNA [1-3]. In the context of the RQC complex, while Ltn1 mediates stalled NC ubiquitylation, Rqc2 mediates their CATylation (in addition to playing a non-essential role in supporting Ltn1 function). Rqc2 residues implicated in CAT tail synthesis are conserved in evolution, suggesting an important function, but the fate of CAT tail-modified proteins had remained unknown. CATylation was not essential for Ltn1-mediated NC degradation (**Figure 2—figure supplement 1B**). Rather, here we report that CATylation promoted formation of NC aggregates—yet another process operating in stalled NC quality control. To our knowledge, this is the first demonstration that proteins can become specifically marked for aggregation.

Although physical characterization of NC aggregates remains to be carried out, evidence presented here indicate shared features with amyloid, including their dependency on a low-complexity aminoacid sequence bearing similarity to polyAla tracts, detergent insolubility, and binding to the J protein, Sis1. With regard to the latter, accumulating evidence suggests that Sis1 may function as an amyloid-recognition factor that enables Ssa- and Hsp104-mediated

disassembly or random fragmentation [28]. This proposed function provides a plausible explanation for our observation that Sis1 depletion led to increased NC aggregate levels, although it remains unclear whether and how regulation of presumably antagonistic Rqc2 and Sis1 activities controls steady-state levels of NC aggregates.

NC aggregation could have different functions, such as in sequestering aberrant NCs into forms less likely to interfere with cellular activities, or in mediating NC elimination *via* vacuolar degradation. Furthermore, NC aggregate formation correlates with the CATylation-dependent activation of Heat Shock Factor 1 (Hsf1) signaling observed in Ltn1-deficient cells [8]. As protein aggregation has been previously shown to elicit Hsf1 activation [29], another conceivable role for NC aggregation is therefore in inducing translational stress signaling. On the other hand, excessive aggregate production certainly has the potential to cause toxicity. With these possibilities in mind, it will be important for future studies to investigate the role of NC aggregation in the neurodegenerative phenotype of Listerin-mutant mice [30].

Materials and Methods

Reagents

Rabbit polyclonal antibodies were: anti-Protein A (Sigma), anti-Sis1 [31], anti-Ydj1 [31], and anti-Ssa1 [32]. Mouse monoclonal antibodies used were anti-Flag tag (M2; Sigma), anti-HA tag (12CA5; Roche), anti-Rpl3 (a gift of J. Warner), anti-GFP (Roche) and anti-Pgk1 (Invitrogen). Secondary antibody was HRP-conjugated (Molecular Probes, Eugene, OR). Doxycycline hydrochloride was from Fischer Scientific (Waltham, MA). The recombinant catalytic core of Usp2cc was a generous gift of R. Kopito [14].

S. cerevisiae strains

All strains used in this work are isogenic to BY4741 (MATa; *his3*Δ1; *leu2*Δ0; *met15*Δ0; *ura3*Δ0) or BY4742 (MATa; *his3*Δ1; *leu2*Δ0; *lys*2Δ0; *ura3*Δ0), except for the experiments shown in **Figure 1—figure supplement 1B**, in which the DS10 strain was used (MATa; *trp1*Δ; *lys1*; *lys2*; *ura3-52*; *leu2-3,112*; *his3-11,15*), and **Figures 3D and 3E**, in which the W303 strain was used (MATa; *leu2-3,112*; *trp1-1*; *can1-100*; *ura3-1*; *ade2-1*; *his3-11,15*). Derivative strains are shown in **Supplementary file 2** (Table SI). Mutant strains carrying single gene deletions were obtained commercially (Thermo Scientific). Additional deletions were performed by using cassettes designed to replace genes of interest with selection markers via homologous recombination. Primers used follow:

LTN1 deletion (using His3MX6 or KanMX6 cassettes):

FWD: 5'
TTGTTTAAAAAATGTAGTACATTTATATGAAATTTATATGCGATAGTCTAGAATTCG
AGCTCGTTTAAAC;

REV: 5'
AAATCTGCTAAGCCATCAAAAAAAGTTCAAGCAATAGTTGGTTCTTAATGCGGATCC
CCGGGTTAATTAA

Growth conditions

Cells were grown at 30° in SD-media. For Sis1 depletion *Sis1*-Tet Off strains were grown in SD-Glu media overnight, diluted in SD-Glu containing 10 μg/ml doxycycline to 0.05 OD_{600} and grown for 12 h. Cells were re-diluted in fresh SD-Glu containing doxycycline and incubated for further 12 h to complete Sis1 deletion. It was necessary to keep the doxycycline incubation time as short as possible, as extended Sis1 depletion caused reduction in cellular growth and viability.

Constructs

The Protein A constructs were a gift of A. van Hoof (UT-Houston) [12]. The Htt-polyQ constructs were gifts of S. Lindquist (Whitehead Institute) [33]. The GFP-R12-RFP (GRR) construct was a gift of O. Brandman (Stanford Univ.) [5]. The K0, NS, and K12 reporters have been described [4,11].

Constructs HA-GFP-stop-R12 ("GFP") and the stalling derivative, HA-GFP-R12-stop ("GFP-R12") were made on pRS316 (*URA3* marker; *CEN*) with the GPD promoter. These constructs

were utilized as the basis for the GFP K-less derivatives: HA-GFP K-less-stop-R12 ("K-less") and HA-GFP K-less-R12-stop ("K-less-R12") by replacing Lys codons in the GFP coding sequence with the preferred Arg AGA or AGG codons through gene synthesis (IDT; sequence below). The R12 stalling sequence utilized unpreferred CGN Arg codons: CGG CGA CGA CGG CGC CGC CGG CGA CGA CGG CGC CGC. For Protein A K-less constructs, HA-tagged Protein A ZZ domain (wild type or K-less; stop codon-containing or non-stop) were generated by gene synthesis (IDT; sequence below) in the same way as the HA-GFP-K-less constructs above, and used to replace the homologous sequence upstream of the hammerhead ribozyme sequence of the PtnA-Rz construct gifted by A. van Hoof (UT-Houston).

HA-GFP R12 - 789 bp

ATGTACCCATACGATGTTCCAGATTACGCTAGTAAAGGAGAAGAACTTTTCACTGGA
GTTGTCCCAATTCTTGTTGAATTAGATGGTGATGTTAATGGGCACAAATTTTCTGTCA
GTGGAGAGGGTGAAGGTGATGCAACATACGGAAAACTTACCCTTAAATTTATTTGC
ACTACTGGAAAACTACCTGTTCCATGGCCAACACTTGTCACTACTCTGACGTATGGT
GTTCAATGCTTTTCCCGTTATCCGGATCATATGAAACGGTATGACTTTTTCAAGAGTG
CCATGCCCGAAGGTTATGTACAGGAACGCACTATATCTTTCAAAGATGACGGGAACT
ACAAGACGCGTGCTGAAGTCAAGTTTGAAGGTGATACCCTTGTTAATCGTATCGAGT
TAAAAGGTATTGATTTTAAAGAAGATGGAAACATTCTCGGACACAAACTCGAGTAC
AACTATAACTCACACAATGTATACATCACGGCAGACAAACAAAAGAATGGAATCAA
AGCTAACTTCAAAATTCGCCACAACATTGAAGATGGATCCGTTCAACTAGCAGACCA
TTATCAACAAAATACTCCAATTGGCGATGGCCCTGTCCTTTTACCAGACAACCATTA
CCTGTCGACACAATCTGCCCTTTTGAAAGATCCCAACGAAAAGCGTGACCACATGGT

CCTTCTTGAGTTTGTAACTGCTGCTGGGATTACACATGGCATGGATGAACTATACAA

AACTAGCCGGCGACGACGGCGCCGCCGGCGACGACGGCGCCGCtgatga

HA-K-less GFP R12 - 789 bp

ATGTACCCATACGATGTTCCAGATTACGCTAGTAgAGGAGAAGAACTTTTCACTGGA

GTTGTCCCAATTCTTGTTGAATTAGATGGTGATGTTAATGGGCACAgATTTTCTGTCA

GTGGAGAGGGTGAAGGTGATGCAACATACGGAAggCTTACCCTTAggTTTATTTGCAC

TACTGGAAgACTACCTGTTCCATGGCCAACACTTGTCACTACTCTGACGTATGGTGTT

CAATGCTTTTCCCGTTATCCGGATCATATGAgACGGTATGACTTTTTCAgaAGTGCCAT

GCCCGAAGGTTATGTACAGGAACGCACTATATCTTTCAgAGATGACGGGAACTACAg

aACGCGTGCTGAAGTCAgGTTTGAAGGTGATACCCTTGTTAATCGTATCGAGTTAAgg

GGTATTGATTTTAgAGAAGATGGAAACATTCTCGGACACAgACTCGAGTACAACTAT

AACTCACACAATGTATACATCACGGCAGACAgACAAAgGAATGGAATCAgAGCTAAC

TTCAggATTCGCCACAACATTGAAGATGGATCCGTTCAACTAGCAGACCATTATCAA

CAAAATACTCCAATTGGCGATGGCCCTGTCCTTTTACCAGACAACCATTACCTGTCG

ACACAATCTGCCCTTTTGAgAGATCCCAACGAAagGCGTGACCACATGGTCCTTCTTG

AGTTTGTAACTGCTGCTGGGATTACACATGGCATGGATGAACTATACcgAACTAGCC

GGCGACGACGGCGCCGCCGGCGACGACGGCGCCGCtgatga

HA-Protein A ZZ domain - 492 bp

ATGTACCCATACGATGTTCCTGACTATGCGGGCTATCCCTATGACGTCCCGGACTAT

GCAGGATCCTATCCATATGACGTTCCAGATTACGCTCCGGCCGCCGCATGCCTTGCG

CAACACGATGAAGCCGTAGAtAAtAAATTCAACAAAGAACAgCAAAAtGCGTTCTAcG

AGATaTTgCATTTgCCTAACTTAAACGAAGAACAACGcAACGCaTTCATaCAAAGTTTg
AAAGATGACCCtAGCCAAAGtGCcAAtCTaTTgGCtGAAGCcAAAAAGCTgAATGATGCa
CAaGCaCCGAAAGTcGACAACAAATTCAACAAAGAACAACAAAACGCGTTCTATGAG
ATCTTACATTTACCTAACTTAAACGAAGAACAGCGAAACGCCTTCATCCAAAGTTTA
AAAGATGACCCAAGCCAAAGCGCTAACCTTTTAGCAGAAGCTAAAAAGCTAAATGA
TGCTCAGgCGCCGAAAGTAGACGCGAATGGA

HA-K-less protein A ZZ domain - 492 bp

ATGTACCCATACGATGTTCCTGACTATGCGGGCTATCCCTATGACGTCCCGGACTAT
GCAGGATCCTATCCATATGACGTTCCAGATTACGCTCCGGCCGCCGCATGCCTTGCG
CAACACGATGAAGCCGTAGAtAAtAgATTCAACAgAGAACAgCAAAAtGCGTTCTAcGA
GATaTTgCATTTgCCTAACTTAAACGAAGAACAACGcAACGCaTTCATaCAAAGTTTgA
gAGATGACCCtAGCCAAAGtGCcAAtCTaTTgGCtGAAGCcAgAAgaCTgAATGATGCaCAa
GCaCCGAgAGTcGACAACAgATTCAACAgAGAACAACAAAACGCGTTCTATGAGATCT
TACATTTACCTAACTTAAACGAAGAACAGCGAAACGCCTTCATCCAAAGTTTAAgAG
ATGACCCAAGCCAAAGCGCTAACCTTTTAGCAGAAGCTAgAAgaCTAAATGATGCTC
AGgCGCCGAgAGTAGACGCGAATGGA

For Rqc2 expression in yeast, the coding sequence of *S. cerevisiae RQC2* was amplified by PCR with the 3xFLAG epitope added at the C-terminus, and cloned into the YCplac111 vector (*LEU2* marker, *CEN*) with the GPD promoter. Mutants were constructed by site-directed mutagenesis using QuikChange Lightning kit (Stratagene, Santa Clara, CA).

Protein expression analyses

MG132 treatment of yeast cells was as described [34]. Total soluble extracts were prepared as described [4]. Protein quantitation was performed by the BCA method. 7.5-30 µg of protein extract were resuspended in 1% SDS, 0.005% bromophenol blue, 5% glycerol, 50 mM dithiothreitol, 50 mM Tris-Cl (pH 6.8) and incubated at 100°C for 5 min before fractionation by gel electrophoresis and immunoblotting.

Usp2-mediated deubiquitylation

30 µg of *ltn1*Δ cell extracts expressing K12 were treated with the recombinant catalytic core of Usp2 (Usp2cc; 5 µM) for 1h at room temperature, as described [14]. The reaction was stopped by adding DTT-containing SDS-PAGE loading buffer and boiling for 3 min.

Aggregate fractionation by high speed centrifugation

Aggregate fractionation was performed as described [15,16] with minor modifications. Briefly, cells were grown to late logarithmic phase (A_{600} = 0.8) and harvested by centrifugation at 2,000 x *g* for 2 min. The cell pellet was resuspended in 750 µL cold non-denaturing lysis buffer [1% Triton, 140 mM NaCl, 1.5 mM $MgCl_2$, EDTA-free protease inhibitor cocktail (Roche), 20 U/mL RNase inhibitor (RNaseOUT, Invitrogen) and 10 mM Tris-Cl (pH 7.4)] and combined with 750 µL of 0.5-mm diameter glass beads. Suspensions were homogenized (three times for 45 s in a FastPrep FP120 Savant homogenizer) and lysates were transferred to clean tubes and centrifuged at 1,000 x *g*, for 10 min at 4°C. Pre-cleared cell extract supernatants (S1) were further fractionated at 16,000 x *g* for another 10 min to pellet aggregates.

436

437 **Co-Immunoprecipitation**

438 Cells were grown to late logarithmic phase (A_{600} = 0.8) and harvested by centrifugation at 2,000
439 x *g* for 2 min. The cell pellet was resuspended in 750 µL of cold non-denaturing lysis buffer
440 [0.2% NP40, 140 mM NaCl, 1.5 mM $MgCl_2$, 1x EDTA-free protease inhibitor cocktail (Roche),
441 20 U/mL of RNase inhibitor (RNaseOUT; Invitrogen) and 10 mM Tris-Cl (pH 7.4)] and
442 combined with 750 µL of 0.5-mm diameter glass beads. Suspensions were homogenized (three
443 times for 45 s in a FastPrep FP120 Savant homogenizer) and lysates were transferred to clean
444 tubes and centrifuged at 2,800 x *g*, for 10 min at 4°C. 1 mg of soluble extract was incubated with
445 1 µg of anti-Flag antibody overnight at 4°C. Next, 600 µg of washed protein G magnetic beads
446 (Life Technologies) were added and incubated for 2 h at 4°C. Beads were pelleted and washed 5
447 times with cold lysis buffer before proteins were eluted by boiling in sample buffer.

448

449 **Immunoprecipitation of K-less aggregates**

450 For the experiment presented in **Figure 4—figure supplement 1**, Cells were grown in SD media
451 lacking uracyl, supplemented with 0.1% proline and 0.003% SDS until OD600 = 0.8, followed
452 by treatment with MG132 (75µM) or DMSO for 2h. Cells were lysed with 2% SDS lysis buffer
453 and extracts were boiled for 3 min. Samples were diluted 20-fold in 0.5% triton lysis buffer and
454 IP'ed with HA-agarose (Sigma) for 3h at 4C before running on SDS-PAGE.

455

456 **Imaging**

For image acquisition and analysis, cells were grown as indicated and harvested by centrifugation and resuspended in PBS. Widefield microscopy was performed with an Olympus xcellence IX81microscope system using a 100x/1.45 NA Plan-Apochromat oil objective lens (Olympus) and a single band GFP filter set (AHF, Germany). As fluorescence light source the illumination system MT20 (Olympus) with a 150 W Xe arc burner was used. Z-stacks of images were recorded with slice distances of 200 nm and displayed as maximum intensity projections. Deconvolution of widefield images from Z-stacks was performed by using the Wiener filter of the Olympus xcellence software. Image processing for final figure preparation was performed with ImageJ (Schneider, C.A., Rasband, W.S., Eliceiri, K.W. "NIH Image to ImageJ: 25 years of image analysis". *Nature Methods* 9, 671-675, 2012). For quantification of phenotypes, several areas with cells were randomly acquired and 45 or more cells were used for the analysis.

Multidimensional Protein Identification Technology (MudPIT) and LTQ mass spectrometry

Exponentially growing cells were collected, washed in cold water and lysed using glass beads in 10 mM Tris-HCl pH 7.4, 140 mM NaCl, 1.5 mM $MgCl_2$ and 0.2% NP40. 40 mg of total protein were used for IP with 40 µg Flag antibody and Protein A Dynabeads for 6h at 4^{o}C. After 4 washes in lysis buffer, proteins were eluted in 200 µl of 300 µg/ml 3X Flag peptide for 30 min, at room temperature. Eluted samples were TCA-precipitated, resuspended in 8M urea, and treated with ProteasMAX (Promega, Madison, WI, USA) per the manufacturer's instruction. Subsequently, samples were reduced by 20 min incubation with 5mM TCEP (*tris*(2 carboxyethyl)phosphine) at room temperature, alkylated in the dark by treatment with 10mM Iodoacetamide for 20 min, and quenched with excess TCEP. Proteins were digested overnight at

37 degrees with Sequencing Grade Modified Trypsin (Promega, Madison, WI, USA) and the reaction was stopped with formic acid.

The protein digest was subjected to cation-exchange microcapillary chromatography, and elutates from the column were electrosprayed directly into an LTQ mass spectrometer (ThermoFinnigan, Palo Alto, CA). A cycle of one full-scan mass spectrum (400-2000 m/z) followed by 7 data-dependent MS/MS spectra at a 35% normalized collision energy was repeated continuously throughout each step of the multidimensional separation. Application of mass spectrometer scan functions and HPLC solvent gradients were controlled by the Xcalibur datasystem.

Protein identification and quantification analysis were done with Integrated Proteomics Pipeline (IP2, Integrated Proteomics Applications, Inc. San Diego, CA). Tandem mass spectra were searched against the *Saccharomyces* Genome Database (SGD) protein database (http://www.yeastgenome.org/download-data/sequence, released on 01-05-2010). LTQ data was searched with 3000.0 milli-amu precursor tolerance and the fragment ions were restricted to a 600.0 ppm tolerance. The ProLuCID search results were assembled and filtered using the DTASelect program (version 2.0) [35,36] with false discovery rate (FDR) of 0.15, under such filtering conditions, the estimated false discovery rate was less than 5.4% at the protein level in each analysis.

Acknowledgments. We thank J. Warner, A. van Hoof, R. Kopito, O. Brandman, and S. Lindquist for reagents. E.B.T. gratefully acknowledges the Brazilian Council for Scientific and Technological Development (CNPq) for a Post-doctoral Fellowship. M.K. was supported by the Hartmut Hoffmann-Berling International Graduate School of Molecular and Cellular Biology (HBIGS). J.N.S. gratefully acknowledges the NRSA for Post-doctoral Fellowship F32AG039127. Work in the Joazeiro laboratory was supported by NIH R01 grants NS075719 from the National Institute of Neurological Disorders and Stroke (NINDS) and CA152103 from the National Cancer Institute (NCI). Work in the Yates laboratory was supported by NIH grants P41 GM103533 and R01 MH067880. Work in the Craig laboratory was supported by NIH R01 grant GM31107 from the National Institute of General Medical Sciences (NIGMS). Work in the Bukau laboratory was supported by a grant of the Deutsche Forschungsgemeinschaft (SFB1036) to B.B. and A.M. This is manuscript 29225 from The Scripps Research Institute.

References

1 Wang, F., Canadeo, L. A. & Huibregtse, J. M. Ubiquitination of newly synthesized proteins at the ribosome. *Biochimie* **114**, 127-133, doi:10.1016/j.biochi.2015.02.006 (2015).

2 Comyn, S. A., Chan, G. T. & Mayor, T. False start: cotranslational protein ubiquitination and cytosolic protein quality control. *J Proteomics* **100**, 92-101, doi:10.1016/j.jprot.2013.08.005 (2014).

3 Lykke-Andersen, J. & Bennett, E. J. Protecting the proteome: Eukaryotic cotranslational quality control pathways. *J. Cell Biol.* **204**, 467-476, doi:10.1083/jcb.201311103 (2014).

4 Bengtson, M. H. & Joazeiro, C. A. Role of a ribosome-associated E3 ubiquitin ligase in protein quality control. *Nature* **467**, 470-473, doi:nature09371 [pii]10.1038/nature09371 (2010).

5 Brandman, O. *et al.* A ribosome-bound quality control complex triggers degradation of nascent peptides and signals translation stress. *Cell* **151**, 1042-1054, doi:10.1016/j.cell.2012.10.044 (2012).

6 Defenouillere, Q. *et al.* Cdc48-associated complex bound to 60S particles is required for the clearance of aberrant translation products. *Proc. Natl. Acad. Sci. U. S. A.* **110**, 5046-5051, doi:10.1073/pnas.1221724110 (2013).

7 Lyumkis, D. *et al.* Structural basis for translational surveillance by the large ribosomal subunit-associated protein quality control complex. *Proc. Natl. Acad. Sci. U. S. A.* **111**, 15981-15986, doi:10.1073/pnas.1413882111 (2014).

8 Shen, P. S. *et al.* Protein synthesis. Rqc2p and 60S ribosomal subunits mediate mRNA-independent elongation of nascent chains. *Science* **347**, 75-78, doi:10.1126/science.1259724 (2015).

9 Shao, S., Brown, A., Santhanam, B. & Hegde, R. S. Structure and assembly pathway of the ribosome quality control complex. *Mol. Cell* **57**, 433-444, doi:10.1016/j.molcel.2014.12.015 (2015).

10 Verma, R., Oania, R. S., Kolawa, N. J. & Deshaies, R. J. Cdc48/p97 promotes degradation of aberrant nascent polypeptides bound to the ribosome. *eLife* **2**, e00308, doi:10.7554/eLife.00308 (2013).

11 Ito-Harashima, S., Kuroha, K., Tatematsu, T. & Inada, T. Translation of the poly(A) tail plays crucial roles in nonstop mRNA surveillance via translation repression and protein destabilization by proteasome in yeast. *Genes Dev.* **21**, 519-524, doi:21/5/519 [pii]10.1101/gad.1490207 (2007).

12 Wilson, M. A., Meaux, S. & van Hoof, A. A genomic screen in yeast reveals novel aspects of nonstop mRNA metabolism. *Genetics* **177**, 773-784, doi:10.1534/genetics.107.073205 (2007).

13 Letzring, D. P., Wolf, A. S., Brule, C. E. & Grayhack, E. J. Translation of CGA codon repeats in yeast involves quality control components and ribosomal protein L1. *RNA* **19**, 1208-1217, doi:10.1261/rna.039446.113 (2013).

14 Kaiser, S. E. *et al.* Protein standard absolute quantification (PSAQ) method for the measurement of cellular ubiquitin pools. *Nature methods* **8**, 691-696, doi:10.1038/nmeth.1649 (2011).

15 Fang, N. N., Ng, A. H., Measday, V. & Mayor, T. Hul5 HECT ubiquitin ligase plays a major role in the ubiquitylation and turnover of cytosolic misfolded proteins. *Nature cell biology* **13**, 1344-1352, doi:10.1038/ncb2343 (2011).

16 Koplin, A. *et al.* A dual function for chaperones SSB-RAC and the NAC nascent polypeptide-associated complex on ribosomes. *J. Cell Biol.* **189**, 57-68, doi:10.1083/jcb.200910074 (2010).

17 Toyama, B. H. & Weissman, J. S. Amyloid structure: conformational diversity and consequences. *Annu. Rev. Biochem.* **80**, 557-585, doi:10.1146/annurev-biochem-090908-120656 (2011).

18 Liebman, S. W. & Chernoff, Y. O. Prions in yeast. *Genetics* **191**, 1041-1072, doi:10.1534/genetics.111.137760 (2012).

19 Krobitsch, S. & Lindquist, S. Aggregation of huntingtin in yeast varies with the length of the polyglutamine expansion and the expression of chaperone proteins. *Proc. Natl. Acad. Sci. U. S. A.* **97**, 1589-1594 (2000).

20 Albrecht, A. & Mundlos, S. The other trinucleotide repeat: polyalanine expansion disorders. *Curr. Opin. Genet. Dev.* **15**, 285-293, doi:10.1016/j.gde.2005.04.003 (2005).

21 Parsell, D. A., Kowal, A. S., Singer, M. A. & Lindquist, S. Protein disaggregation mediated by heat-shock protein Hsp104. *Nature* **372**, 475-478, doi:10.1038/372475a0 (1994).

22 Mogk, A., Kummer, E. & Bukau, B. Cooperation of Hsp70 and Hsp100 chaperone machines in protein disaggregation. *Frontiers in molecular biosciences* **2**, 22, doi:10.3389/fmolb.2015.00022 (2015).

23 Nillegoda, N. B. *et al.* Crucial HSP70 co-chaperone complex unlocks metazoan protein disaggregation. *Nature* **524**, 247-251, doi:10.1038/nature14884 (2015).

24 Aron, R., Higurashi, T., Sahi, C. & Craig, E. A. J-protein co-chaperone Sis1 required for generation of [RNQ+] seeds necessary for prion propagation. *EMBO J.* **26**, 3794-3803, doi:10.1038/sj.emboj.7601811 (2007).

25 Park, S. H. *et al.* PolyQ proteins interfere with nuclear degradation of cytosolic proteins by sequestering the Sis1p chaperone. *Cell* **154**, 134-145, doi:10.1016/j.cell.2013.06.003 (2013).

26 Yang, Z., Hong, J. Y., Derkatch, I. L. & Liebman, S. W. Heterologous gln/asn-rich proteins impede the propagation of yeast prions by altering chaperone availability. *PLoS Genet* **9**, e1003236, doi:10.1371/journal.pgen.1003236 (2013).

27 Sokalingam, S., Raghunathan, G., Soundrarajan, N. & Lee, S. G. A study on the effect of surface lysine to arginine mutagenesis on protein stability and structure using green fluorescent protein. *PLoS One* **7**, e40410, doi:10.1371/journal.pone.0040410 (2012).

28 Harris, J. M., Nguyen, P. P., Patel, M. J., Sporn, Z. A. & Hines, J. K. Functional diversification of hsp40: distinct j-protein functional requirements for two prions allow for chaperone-dependent prion selection. *PLoS Genet* **10**, e1004510, doi:10.1371/journal.pgen.1004510 (2014).

29 Zou, J., Guo, Y., Guettouche, T., Smith, D. F. & Voellmy, R. Repression of heat shock transcription factor HSF1 activation by HSP90 (HSP90 complex) that forms a stress-sensitive complex with HSF1. *Cell* **94**, 471-480 (1998).

30 Chu, J. *et al.* A mouse forward genetics screen identifies LISTERIN as an E3 ubiquitin ligase involved in neurodegeneration. *Proc. Natl. Acad. Sci. U. S. A.* **106**, 2097-2103, doi:0812819106 [pii]10.1073/pnas.0812819106 (2009).

31 Yan, W. & Craig, E. A. The glycine-phenylalanine-rich region determines the specificity of the yeast Hsp40 Sis1. *Mol. Cell. Biol.* **19**, 7751-7758 (1999).

32 Lopez-Buesa, P., Pfund, C. & Craig, E. A. The biochemical properties of the ATPase activity of a 70-kDa heat shock protein (Hsp70) are governed by the C-terminal domains. *Proc. Natl. Acad. Sci. U. S. A.* **95**, 15253-15258 (1998).

33 Alberti, S., Halfmann, R., King, O., Kapila, A. & Lindquist, S. A systematic survey identifies prions and illuminates sequence features of prionogenic proteins. *Cell* **137**, 146-158, doi:10.1016/j.cell.2009.02.044 (2009).

34 Liu, C., Apodaca, J., Davis, L. E. & Rao, H. Proteasome inhibition in wild-type yeast Saccharomyces cerevisiae cells. *Biotechniques* **42**, 158, 160, 162 (2007).

35 Cociorva, D., D, L. T. & Yates, J. R. Validation of tandem mass spectrometry database search results using DTASelect. *Curr Protoc Bioinformatics* **Chapter 13**, Unit 13 14, doi:10.1002/0471250953.bi1304s16 (2007).

36 Tabb, D. L., McDonald, W. H. & Yates, J. R., 3rd. DTASelect and Contrast: tools for assembling and comparing protein identifications from shotgun proteomics. *J Proteome Res* **1**, 21-26 (2002).

Figure 1. Stalled translation can lead to the formation of nascent chain aggregates.

(**A**) *Top panels*, diagrams of reporter constructs encoding stalling-prone nascent chains and respective controls. PolyLys-dependent stalling (*left*): GFP-Flag-*HIS3* fusion protein control (K0), its *bona fide* nonstop (NS) protein derivative, and a derivative fused to 12 lysines (K12). Endonucleolytic mRNA cleavage-dependent stalling (*middle*): Protein A ZZ domain-(Ribozyme)-GFP fusion constructs. A self-cleaving ribozyme (Rz) within coding sequence generates a nonstop (NS) mRNA encoding stalled Protein A (PtnA). Controls are constructs with a cleavage-defective ribozyme generating a full-length PtnA-GFP fusion (*rz*), or with a stop codon preceding the Rz cleavage site (STOP-Rz), such that nascent PtnA is not expected to become stalled in ribosomes. Horizontal lines represent the encoded polypeptides. Arg CGN codon-dependent stalling (*right*): GFP-R12-RFP (GRR), where R12 is encoded by unpreferred Arg codons. *Lower panels*, reporter protein expression in a wild type strain (WT; BY4741), a *LTN1*-deleted strain (*ltn1*Δ) or a strain whose endogenous Ltn1 lacks the RING domain (Ltn1 ΔR). Immunoblots of SDS-boiled cell extracts: anti-Flag, anti-PtnA, or anti-GFP to monitor reporter expression, and anti-Pgk1 as loading control. The migration of CATylated species is indicated. Asterisks indicate bands of unknown identity. (**B**) Stalling reporter slow-migrating species are pelleted upon high speed centrifugation. The extract of a K12 reporter-expressing *ltn1*Δ strain was pre-cleared by centrifugation at 1,000 x *g* for 5 min and its supernatant (S1) was then subjected to 16,000 x *g* for 10 min. The resulting supernatant (S16) and pellet (P16) were analyzed by western blot against Flag tag (K12), Rpl3 (a 60S ribosomal protein), Pgk1 (phosphoglycerate kinase 1, a soluble protein) and ubiquitin (high-molecular weight conjugates migrating above 120 kDa are shown). (**C**) Translational stalling is required for reporter

633 aggregation. NS and K12 reporter protein expression in strains lacking Ltn1 and/or the
634 translational stalling factor, Hel2.

635
636

637 **Figure 2. Rqc2-mediated modification of stalled nascent chains with CAT tails results in**
638 **their aggregation.**

639

640 (**A**) NC CATylation correlates with aggregation—effects of *RQC1* and *RQC2* deletion. The
641 indicated strains were transformed with the PtnA NS-Rz reporter. Reporter expression was
642 monitored by immunoblot anti-PtnA. The migration of CATylated species is indicated. (**B**) An
643 Rqc2 mutant defective in CAT tail synthesis fails to promote aggregation of stalled NCs. The
644 *ltn1*Δ *rqc2*Δ strain expressing the GRR reporter was transformed with plasmids encoding Rqc2-
645 Flag wild type (WT) or D98Y mutant. (**C**) Endogenous Rqc2 is limiting for NC CATylation and
646 aggregation in *ltn1*Δ cells. The *ltn1*Δ strain expressing the GRR reporter was transformed or not
647 with plasmid encoding Rqc2-Flag wild type (WT). Reporter expression was monitored by
648 immunoblot anti-GFP. (**D**) Fusion of a CAT tail-mimetic sequence to the C-terminus of the K0
649 reporter protein suffices to promote aggregation independently of stalling or Rqc2. *Top panel*,
650 diagram of constructs. *Lower panel*, as in "a." The indicated strains were transformed with
651 plasmids encoding the parental reporter (K0, as described in 1a) or its derivatives fused to a C-
652 terminal tail of 20 Ala, 20 Thr, or 10 Ala-Thr repeats, as indicated. (**E**) *Punctae* formed by
653 stalling reporters in intact cells correlate with aggregates observed in WCE. Fluorescence
654 microscopy imaging of indicated strains expressing the GRR reporter. GFP-positive *punctae* can
655 be observed in the *ltn1*Δ strain. (**F**) CAT tail-dependent incorporation of the GRR stalling
656 reporter into *punctae*. *Left*, The *ltn1*Δ *rqc2*Δ strain was transformed with plasmids encoding

Rqc2-Flag wild type (WT) or D98Y mutant as in panel "B" and examined by fluorescence microscopy. Three different distribution patterns of the GFP signal that are representative for each strain are shown. Arrows point to selected *punctae*. Scale bar, 2 μm. *Right*, Quantification of cells harboring GFP-positive inclusions in the *ltn1*Δ *rqc2*Δ strains expressing Rqc2 WT or D98Y mutant.

Figure 3. Sis1 association reveals endogenous stalled nascent chain aggregates.

(**A**) Stalling reporters co-IP with Sis1 in an Rqc2-dependent manner. Whole cell extracts (WCE) of the indicated strains were Flag IP'ed (to pull down K0 or K12 reporters), followed by immunoblotting as indicated to the left of the panels. (**B**) Sis1 associates tightly with Rqc2-dependent aggregates formed by endogenous proteins in cells deficient for Ltn1 or Rqc1. WCE of the indicated strains were immunoblotted against Sis1, Ssa1, and Ydj1, as indicated. The ~47 kDa band in the Sis1 blot (asterisk) is nonspecific. (**C**) The formation of slow-migrating Sis1 species is dependent on Rqc2's ability to synthesize CAT tails. WCE of the *ltn1*Δ *rqc2*Δ strain expressing Rqc2-Flag wild type or D98Y mutant were analyzed by immunoblotting. (**D**) Sis1 depletion increases NC aggregation. *ltn1*Δ tetO7-Sis1 cells expressing the K12 stalling reporter were treated or not with doxycycline (DOX). WCE were analyzed by immunoblot against Sis1 (*left panel*) or Flag (*right panel*; for K12 detection). *Asterisk*, cross-reacting band. (**E**) Sis1 depletion increases GFP *punctae* formation in *ltn1*Δ cells. *ltn1*Δ WT-Sis1 or *ltn1*Δ tetO7-Sis1 cells expressing the GRR stalling reporter were grown for 24h in the presence (+) or absence (-) of doxycycline (DOX). *Top*, Three representative images are presented for each strain and treatment condition. Scale bar, 2 μm. Arrows point to selected *punctae*. *Bottom*, Quantification

of cells harboring GFP *punctae*. Is represented by red bars; among those, the fraction of cells with 1 or 2 *punctae* is represented in dark gray, and the fraction of cells with 3 or more *punctae*, in light gray.

Figure 4. Evidence for stalled nascent chain modification with CAT tails and aggregation in wild type cells.

(**A**) Stalling Lys-less reporter modification with CAT tails in wild type yeast. All constructs were HA-tagged. Expression of GFP, GFP-R12, GFP K-less ("K-less"), or GFP K-less R12 ("K-less-R12") reporter proteins in the indicated strains, revealed by anti-HA immunoblot. "R12" is the stalling signal, consisting of 12 suboptimal Arg CGN codons. GFP-R12 expression in *ltn1*Δ cells is used as a control for aggregate formation. *Lower panel*, shorter exposure to reveal relative steady-state levels of monomeric reporter species. (**B**) Stalling PtnA-Rz reporter CATylation and aggregation in wild type yeast. All constructs were HA-tagged. Expression of PtnA-STOP-Rz, PtnA-Rz, PtnA-STOP-Rz K-less, and PtnA-Rz K-less reporter proteins in the wild type strain, revealed by anti-HA immunoblot.

Figure 1—figure supplement 1. Stalled translation can lead to the formation of nascent chain aggregates.

(**A**) The slow migration of stalling reporters expressed in *ltn1*Δ cells is not due to poly-ubiquitylation. Strains utilized were wild type (WT), *ltn1*Δ cells, and *ltn1*Δ cells expressing the K12 reporter. Cell extracts were treated with the recombinant catalytic core of Usp2 (Usp2cc), which has general deubiquitylase activity, for 1h at room temperature, as described [14]. The anti-Flag blot shows a lack of effect of Usp2cc on the migration of high molecular weight stalling reporter species (compare lanes 3 and 6) while the anti-ubiquitin blot confirms that the enzyme was able to efficiently disassemble ubiquitin chains linked to proteins in the extract. (**B**) Loss of *LTN1* is not generally associated with increased formation of protein aggregates. Expression of GFP-Huntingtin exon 1 polyglutamine reporters (Htt-Q25 and Htt-Q72) in WT and *ltn1*Δ strain extracts revealed by anti-GFP immunoblot.

Figure 2—figure supplement 1. Rqc2-mediated modification of stalled nascent chains with CAT tails results in their aggregation.

(**A**) Accumulation of stalling reporters by proteasome inhibition is not sufficient to result in aggregation. Immunoblot analysis of K0 and NS reporter expression in wild type or *ltn1*Δ strains, after treatment (+) or not (-) with the proteasome inhibitor MG132 for 2h. (**B**) The Rqc2 D98Y mutant is competent to support Ltn1 function. Stalling reporter expression in wild type or *rqc2*Δ strains transformed with empty vector, wild type Rqc2-Flag, or Rqc2-Flag D98Y. (**C**) CATylation is required for aggregation of the NS reporter. The *ltn1*Δ *rqc2*Δ strain expressing the

NS reporter was transformed with plasmids encoding Rqc2-Flag wild type (WT) or D98Y mutant. Expression of NS monomers, NS aggregates, and Rqc2-Flag revealed by anti-Flag immunoblot. Panels with different exposure times shown. (**D**) Loss of *RQC2* is not generally associated with the failure to form protein aggregates. Expression of GFP-Huntingtin exon 1 polyglutamine reporters (Htt-Q25 and Htt-Q103) in the indicated strains revealed by anti-GFP immunoblot. (**E**) Stalling reporter aggregates do not form post-lysis. K12 reporter-expressing strains (labeled in red) were mixed 1:1 with a second, untransformed strain (labeled in blue) before lysis, and extracts were analyzed for aggregate formation by anti-Flag immunoblot. The presence of the *ltn1*Δ strain constituents during lysis was not sufficient to promote aggregation of the K12 reporter expressed in a *ltn1*Δ *rqc2*Δ strain (lane 2). Conversely, the presence of constituents of the *ltn1*Δ *rqc2*Δ strain did not interfere with aggregates formed by K12 reporter-expressing *ltn1*Δ strain (compare lane 4 to lane 1).

Figure 3—figure supplement 1. Sis1 association reveals endogenous stalled nascent chain aggregates.

(**A**) The stalling reporters NS and K12, but not the parental K0, co-IP with Sis1. Whole cell extracts (WCE) of *ltn1*Δ strains expressing the indicated reporters were subjected to Flag IP, and analyzed by anti-Sis1 (or Flag control) immunoblot. (**B**) The migration of the high molecular weight Sis1 species present in *ltn1*Δ cells is not affected by treatment with a deubiquitylating enzyme (see Figure1—figure supplement 1A). Extracts from the indicated strains were treated with Usp2cc and analyzed by anti-Sis1 immunoblot. (**C**) Sis1 aggregates co-IP with stalling

reporters. Extracts of Ltn1-deficient cells, untransformed or expressing the K12 reporter, were used for Flag IP (to pull down K12) and immunoblotted against Sis1 or Flag tag, as indicated. *Asterisk*, nonspecific band.

Figure 3—figure supplement 2. *tetO7* promoter-dependent Sis1 depletion.

ltn1Δ tetO7-SIS1 and *ltn1Δ* WT-*SIS1* cells were treated with doxycycline as indicated, and analyzed by western blot using antibodies against Sis1.

Figure 4—figure supplement 1. Stalling NC reporter aggregation in wild type yeast.

HA-tagged GFP, GFP-R12, GFP K-less ("K-less"), or GFP K-less R12 ("K-less R12") reporters expressed in the MG132-treated wild type strain (or MG132 treated *rqc2*Δ strain as a control, lane 5) were concentrated by anti-HA IP and analyzed by anti-HA immunoblot. *Lower panel*, the monomeric forms are shown in a shorter exposure to reveal relative steady-state levels of monomeric reporter species, as well as CAT tails in lane 4.

Supplementary file 1 (Table SI). Mass spectrometry analysis of chaperones co-IP'ed with K0 (stop codon-containing control) and K12 (stalling) reporters from the *ltn1*Δ strain.

K0 and K12 reporters were Flag IP'ed from WCE and analyzed by mass spectrometry. Peptide counts of co-IP'ed chaperones are shown. As represented in diagrams in Figure 1A, the K0 and K12 reporters consist of a GFP-Flag-*HIS3* backbone. Thus, *HIS3* peptide counts, which were the most abundant in the analyses, are presumed to be derived from the IP'ed reporter. We note that these analyses have limited ability to distinguish among homologous proteins with high degree of similarity, such as Ssa1/Ssa2, Hsc82/Hsp82, and Ssb1/Ssb2.

Supplementary file 2 (Table SI). Strain genotypes.

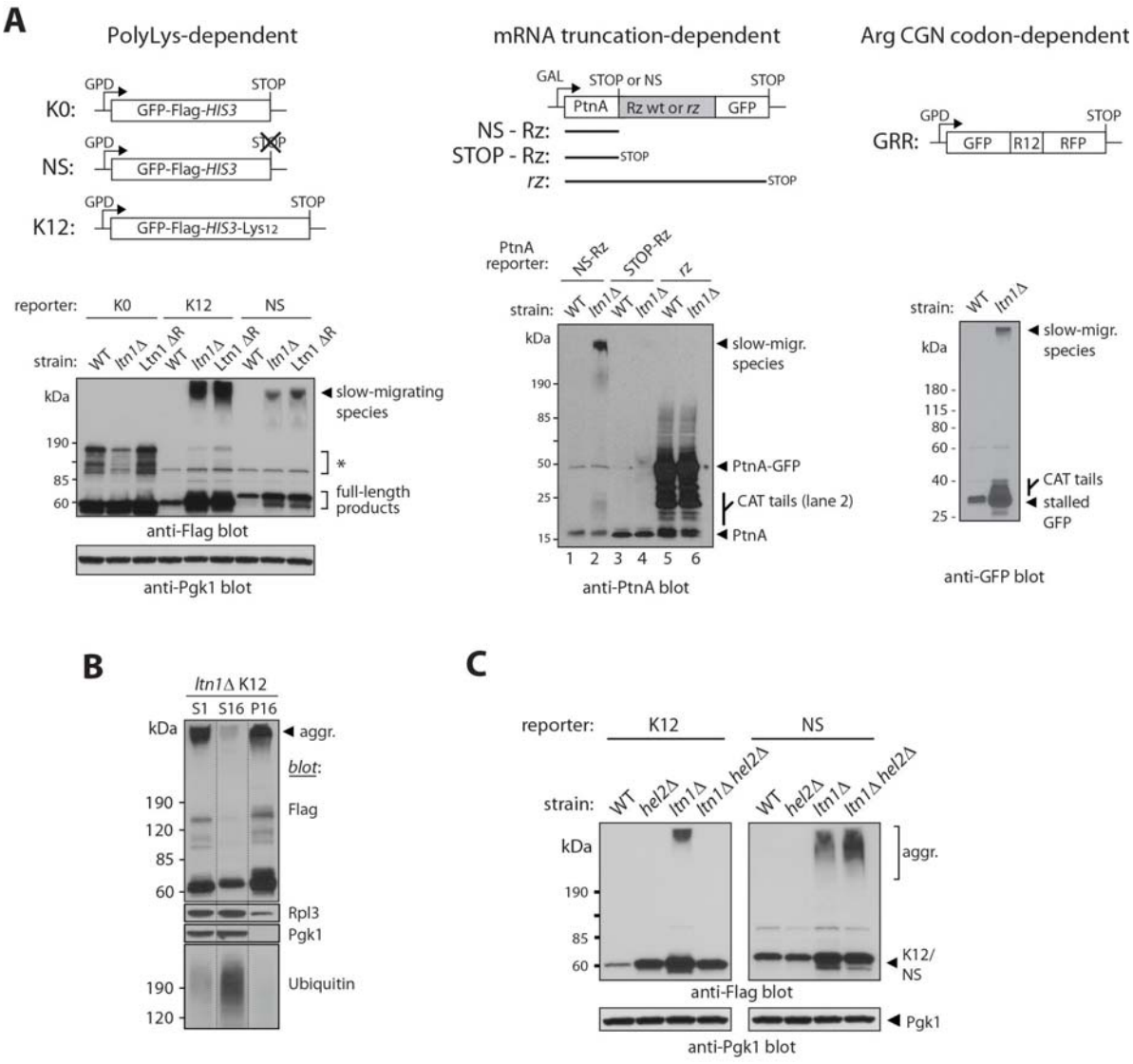
A
PolyLys-dependent
mRNA truncation-dependent
Arg CGN codon-dependent
GPD
STOP
K0:
GFP-Flag-HIS3
NS:
K12:
GFP-Flag-HIS3-Lys12
GAL
STOP or NS
PtnA
Rz wt or rz
GFP
NS - Rz:
STOP - Rz:
rz:
GRR:
R12
RFP
reporter:
K0
K12
NS
strain:
WT
ltn1Δ
Ltn1 ΔR
kDa
190
85
60
slow-migrating species
*
full-length products
anti-Flag blot
anti-Pgk1 blot
PtnA reporter:
NS-Rz
STOP-Rz
rz
slow-migr. species
PtnA-GFP
CAT tails (lane 2)
PtnA
1 2 3 4 5 6
anti-PtnA blot
180
115
80
60
40
25
CAT tails
stalled GFP
anti-GFP blot
B
ltn1Δ K12
S1 S16 P16
aggr.
blot:
Flag
120
Rpl3
Pgk1
Ubiquitin
C
hel2Δ
ltn1Δ hel2Δ
aggr.
K12/ NS
Pgk1

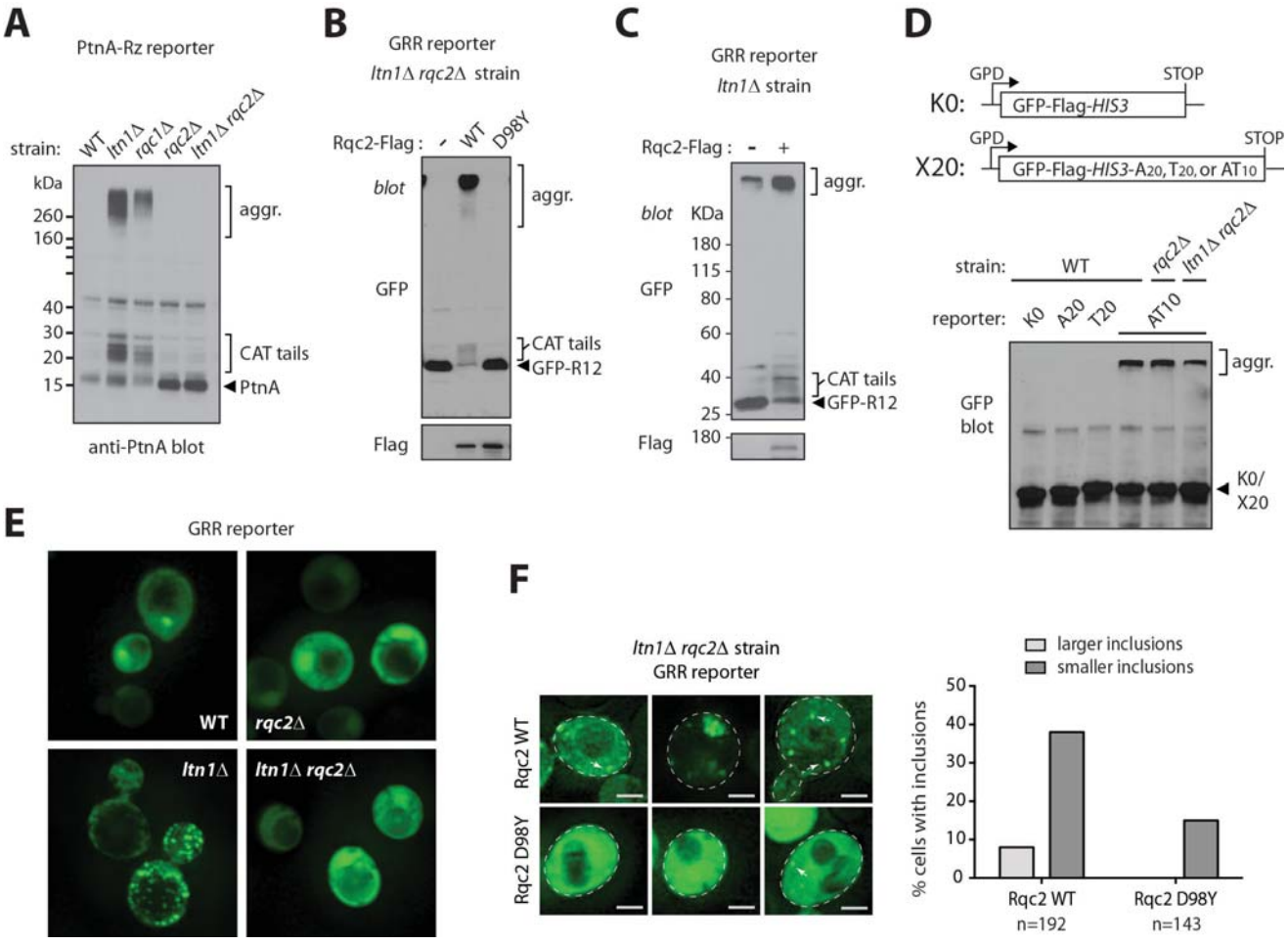
A
PtnA-Rz reporter
strain: WT ltn1Δ rqc1Δ rqc2Δ ltn1Δ rqc2Δ
kDa
260
160
40
30
20
15
aggr.
CAT tails
PtnA
anti-PtnA blot
B
GRR reporter
ltn1Δ rqc2Δ strain
Rqc2-Flag : - WT D98Y
blot
GFP
Flag
aggr.
CAT tails
GFP-R12
C
GRR reporter
ltn1Δ strain
Rqc2-Flag : - +
blot KDa
GFP
Flag
180
115
80
60
40
25
180
aggr.
CAT tails
GFP-R12
D
GPD
STOP
K0: GFP-Flag-HIS3
X20: GFP-Flag-HIS3-A20, T20, or AT10
strain: WT rqc2Δ ltn1Δ rqc2Δ
reporter: K0 A20 T20 AT10
GFP blot
aggr.
K0/ X20
E
GRR reporter
WT
rqc2Δ
ltn1Δ
ltn1Δ rqc2Δ
F
ltn1Δ rqc2Δ strain
GRR reporter
Rqc2 WT
Rqc2 D98Y
larger inclusions
smaller inclusions
% cells with inclusions
50
40
30
20
10
0
Rqc2 WT
n=192
Rqc2 D98Y
n=143

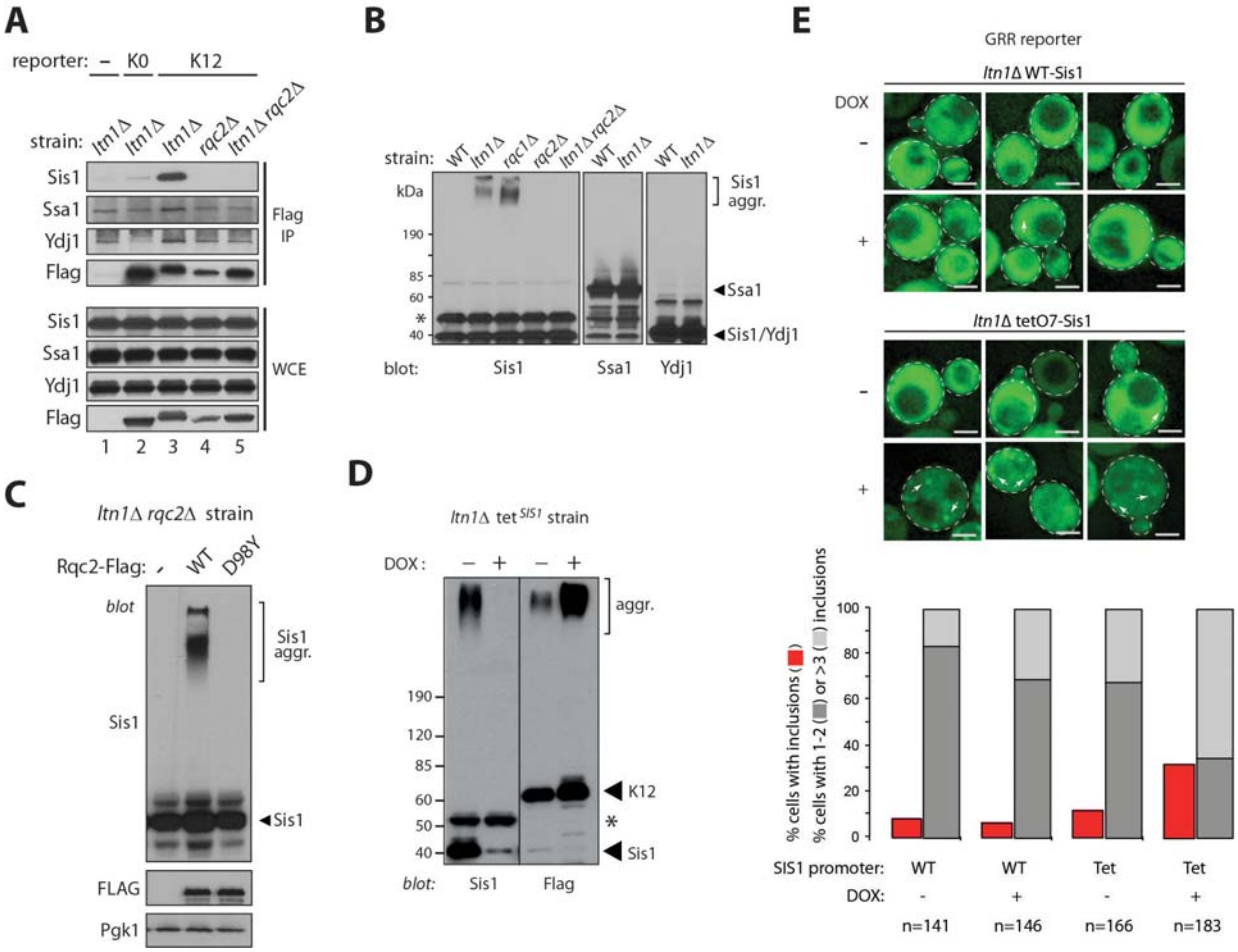
A
reporter: – K0 K12
strain: ltn1Δ ltn1Δ ltn1Δ rqc2Δ ltn1Δ rqc2Δ
Sis1
Ssa1
Ydj1
Flag
Flag IP
Sis1
Ssa1
Ydj1
Flag
WCE
1 2 3 4 5
B
strain: WT ltn1Δ rqc1Δ rqc2Δ ltn1Δ rqc2Δ WT ltn1Δ WT ltn1Δ
kDa
190
85
60
*
40
Sis1 aggr.
Ssa1
Sis1/Ydj1
blot: Sis1 Ssa1 Ydj1
C
ltn1Δ rqc2Δ strain
Rqc2-Flag: - WT D98Y
blot
Sis1 aggr.
Sis1
Sis1
FLAG
Pgk1
D
ltn1Δ tet SIS1 strain
DOX: – + – +
aggr.
190
120
85
60
50
40
K12
*
Sis1
blot: Sis1 Flag
E
GRR reporter
ltn1Δ WT-Sis1
DOX
-
+
ltn1Δ tetO7-Sis1
-
+
% cells with inclusions ( )
% cells with 1-2 ( ) or >3 ( ) inclusions
100
80
60
40
20
0
SIS1 promoter: WT WT Tet Tet
DOX: - + - +
n=141 n=146 n=166 n=183

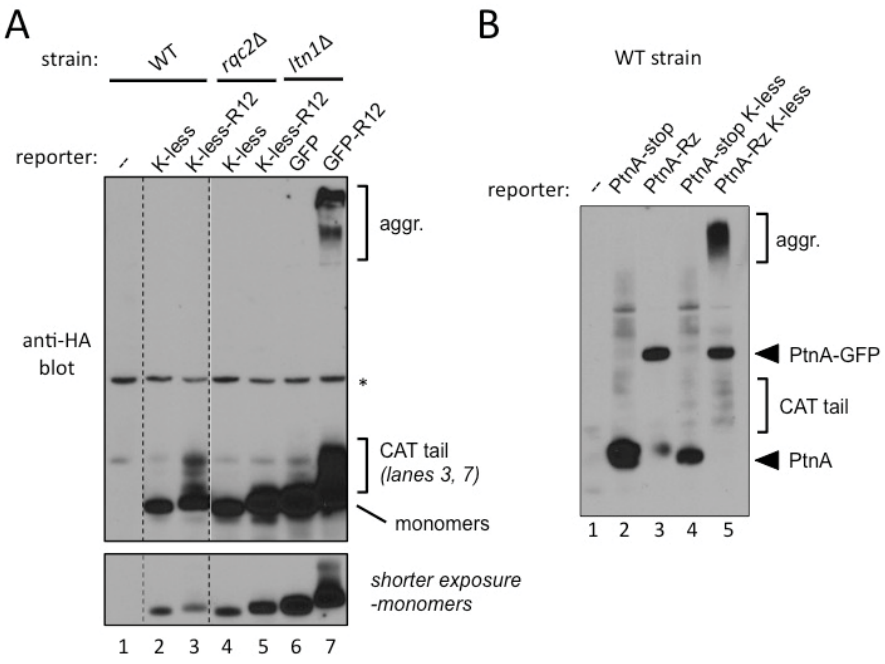
A
strain:
WT
rqc2Δ
ltn1Δ
reporter:
–
K-less
K-less-R12
K-less
K-less-R12
GFP
GFP-R12
anti-HA
blot
aggr.
*
CAT tail
(lanes 3, 7)
monomers
shorter exposure
-monomers
1 2 3 4 5 6 7
B
WT strain
reporter:
–
PtnA-stop
PtnA-Rz
PtnA-stop K-less
PtnA-Rz K-less
aggr.
PtnA-GFP
CAT tail
PtnA
1 2 3 4 5